Stereo-Specific Inhibition of Acetyl- and Butyryl-Cholinesterases by Enantiomers of *Cis,Cis*-Decahydro-2-naphthyl-N-*n*-butylcarbamate

Ming-Cheng Lin,[1] *Shyh-Jei Yeh,*[2] *I-Ru Chen,*[2] *and Gialih Lin*[2]

[1]Department of Internal Medicine, Chung Shan Medical University Hospital and School of Medicine, Chung Shan Medical University, Taichung 402, Taiwan

[2]Department of Chemistry, National Chung-Hsing University, Taichung 402, Taiwan; *E-mail: gilin@dragon.nchu.edu.tw.*

Received 16 February 2011; revised 21 March 2011; accepted 4 April 2011

ABSTRACT: Enantiomers of *cis,cis*-decahydro-2-naphthyl-N-*n*-butylcarbamate show stereo-specific inhibition for acetylcholinesterase and butyryl-cholinesterase. For both inhibition reaction, (2*S*,4a*R*,8a*S*)-*cis,cis*-decahydro-2-naphthyl-N-*n*- butyl-carbamate is more potent than (2*R*,4a*S*,8a*R*)-*cis,cis*-decahydro-2-naphthyl-N-*n*-butylcarbamate. Optically pure (2*S*,4a*R*,8a*S*)-(−)- and (2*R*,4a*S*,8a*R*)-(+)-*cis,cis*-decahydro-2-naphthols are resolved by the porcine pancreatic lipase-catalyzed acetylation of decahydro-2-naphthols with vinyl acetate. Absolute configurations and the enantiomeric excess values of (2*S*,4a*R*,8a*S*)-(−)- and (2*R*,4a*S*,8a*R*)-(+)-*cis,cis*-decahydro-2-naphthols are determined from the ^{19}F NMR spectra of their Mosher's ester derivatives. We fail to resolve (2*S*,4a*R*,8a*R*)- and (2*R*,4a*S*,8a*S*)-*trans,cis*-decahydro-2-naphthols from the porcine pancreatic lipase-catalyzed acetylation of decahydro-2-naphthols with vinyl acetate. © 2011 Wiley Periodicals, Inc. J Biochem Mol Toxicol 25:330–339, 2011; View this article online at wileyonlinelibrary.com. DOI 10:1002/jbt.20394

KEYWORDS: **Acetylcholinesterase; Butyrylcholinesterase; Carbamate Inhibitor; Stereospecificity**

INTRODUCTION

Two forms of cholinesterase coexist ubiquitously throughout the body, acetylcholinesterase (AChE, EC 3.1.1.7) [1–3] and butyrylcholinesterase (BChE, EC 3.1.1.8) [4–7], and although highly homologous, >65%, they are products of different genes on chromosomes 7 and 3 in humans, respectively. Both subtype unselective cholinesterase and human AChE-selective inhibitors have been used in Alzheimer's disease to amplify the action of acetylcholine at remaining cholinergic synapses within the Alzheimer's disease brain. The X-ray crystal structures of *Torpedo californica* AChE have revealed that the enzyme contains a catalytic triad similar to that present in other serine hydrolases. It has also revealed that this triad is located near the bottom of a deep and narrow gorge about 20 Å in depth [2]. The X-ray crystal structure of human BChE has been reported [4,5,7]. *T. californica* AChE and human BChE have a common catalytic triad, Ser–His–Glu. The active sites of both enzymes are located at the bottom of a cavity and act as nucleophiles to attack the carbonyl groups of substrates or pseudosubstrate inhibitors.

Carbamate inhibitors, such as Alzheimer's disease drug Rivastigmine (Exelon) (Figure 1) and aryl carbamates, are characterized as the pseudosubstrate inhibitors of AChE, BChE, cholesterol esterase, and lipase [3,8–15]. In the presence of substrate, the kinetic schemes for pseudosubstrate inhibitions of serine hydrolases by carbamate inhibitors have been illustrated (Figure 2) [8]. These reactions are going on simultaneously, with the inhibitor and substrate competing for the active site of the enzyme. In addition, reactivation of the enzyme is insignificant when compared to carbamylation of the enzyme and therefore the k_3 values can be ignored ($k_2 \gg k_3$). Equation (1) is the solution of differential equation that describes the set of reactions depicted in Figure 2. In Eq. (1), the k_{app} values are first-order rate constants, which are obtained by Hosie's method.

$$k_{app} = k_2[I]/(K_i(1 + [S]/K_m) + [I]) \quad (1)$$

Therefore, the K_i and k_2 values are obtained as parameters from the nonlinear least squares of curve fittings

Correspondence to: Gialih Lin.
Contract Grant Sponsor: National Council of Taiwan.

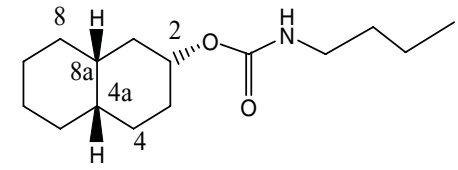

(2R,4aS,8aR)-cis,cis-decahydro-2-naphthyl-N-*n*-butylcarbamate

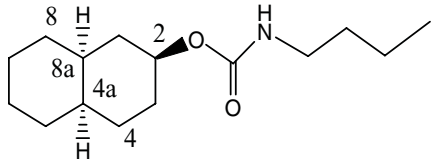

(2S,4aR,8aS)-cis,cis-decahydro-2-naphthyl-N-*n*-butylcarbamate

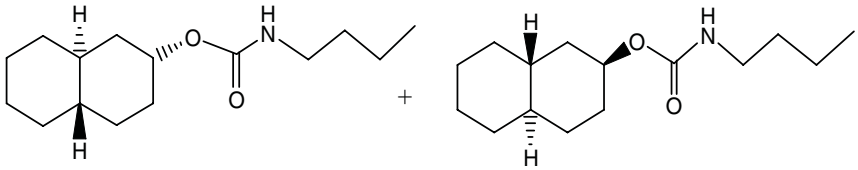

racemic-*trans,cis*-decahydro-2-naphthyl-N-*n*-butylcarbamate

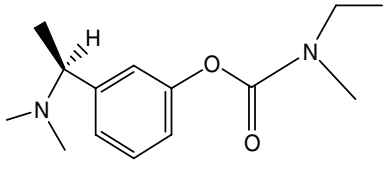

Rivestigmine

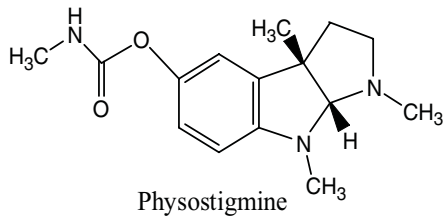

Physostigmine

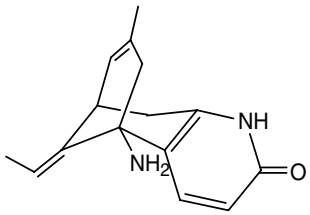

Huperzine-A

FIGURE 1. Structures of (2*S*,4a*R*,8a*S*)- and (2*R*,4a*S*,8a*R*)-*cis,cis*-decahydro-2-naphthyl-N-*n*-butylcarbamate, racemic (±)-*trans,cis*-decahydro-2-naphthyl- N-*n*-butylcarbamate, Rivatigmine, Physostigmine, and Huperzine-A.

of k_{app} vs. inhibitor concentration ([I]) following Eq. (1). The bimolecular rate constant, $k_i = k_2 / K_i$, is defined as the overall inhibitory potency.

The stereospecificity of AChE plays an important role in many Alzheimer's disease drug such as Rivastigmine, Physostigmine, and Huperzine-A (Figure 1). We have reported that AChE has shown stereo-specific inhibition for stereoisomers of 1,1′-bi-2-naphthyl-di-N-*n*-butylcarbamate [16] and *exo*- and *endo*-2-norbornyl-N-*n*-butylcarbamates [17]. BChE has also shown stereo-specific inhibition by enantiomers of isomalathion [18], *exo*- and *endo*-2-norbornyl-N-*n*-butylcarbamates [19]. In this paper, we further synthesized optically pure (2*S*,4a*R*,8a*S*)- and (2*R*,4a*S*,8a*R*)-*cis,cis*-decahydro-2-naphthyl-N-*n*-carbamates from (2*S*,4a*R*,8a*S*)-(−)- and (2*R*,4a*S*,8a*R*)-(+)- *cis,cis*-decahydro-2-naphthols to probe stereospecificity for both AChE and BChE inhibitions (Figure 1).

Optically pure (2*S*,4a*R*,8a*S*)-(−)- and (2*R*,4a*S*,8a*R*)-(+)- *cis,cis*-decahydro-2-naphthols have been resolved from microbial hydrolysis of (±)-*cis,cis*-decahydro-2-naphthyl acetate by *Bacillus subtilis* [20]. For resolution of enantiomers of secondary alcohols, lipases (EC 3.1.1.3) have been widely chosen to use because lipases can be applied in

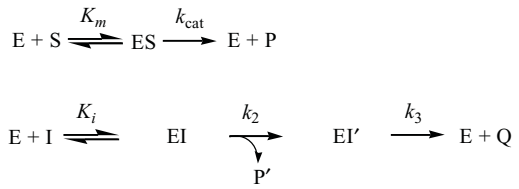

FIGURE 2. Kinetic scheme for the pseudosubstrate inhibition of butyrylcholinesterase by carbamate inhibitors in the presence of substrate. E, enzyme; S, substrate butyrylthiocholine; ES, acylenzyme intermediate; I, carbamate, EI, enzyme-inhibitor tetrahedral intermediate; EI′, carbamyl enzyme intermediate; P, thiocholine from the substrate reaction; P′, alcohol-leaving groups from the pseudosubstrate inhibition, Q, carbamic acids.

organic solvent that is very convenient to organic chemists [21,22]. In this paper, we apply the lipase-catalyzed stereospecifically acetylation of one of enantiomers of (2*S*,4a*R*,8a*S*)-(−)- and (2*R*,4a*S*,8a*R*)-(+)-*cis*,*cis*-decahydro-2-naphthols form a mixture of stereoisomers of decahydro-2-naphthols with vinyl acetate (Figure 3).

MATERIALS AND METHODS

Materials

All chemicals were of the highest grade available. Silica gel used in liquid chromatography and thin-layer chromatography plates were obtained from Merck, Darmstadt, Germany. Horse serum BChE, butyrylthiocholine, and 5,5′-dithio-bis(2-nitrobenzoic acid) (DTNB) were obtained from Sigma, St. Louis, Missouri, USA.

Chemistry

Synthesis

Kinetic Resolution of (2S,4aR,8aS)-(−)- and (2R,4aS,-8aR)-(+)-cis,cis- decahydro-2-naphthols. To a *t*-butyl methyl ether (50 mL) solution of decahydro-2-naphthol (32.5 mmol.) and vinyl acetate (10 mL), 30 g of porcine pancreatic lipase were added. The reaction mixture was shaken at 37°C at 200 rpm for 72 h. This reaction yielded (2*S*,4a*R*,8a*S*)-(−)-*cis*,*cis*-decahydro-2-naphthyl acetate (33%) and recovered unreactive (2*R*,4a*S*,8a*R*)-(+)-*cis*,*cis*-decahydro-2-naphthol (35%) and racemic (±)-*trans*,*cis*-decahydro-2-naphthol (30%) (Figure 3a). The optical purity of (2*R*,4a*S*,8a*R*)-(+)-*cis*,*cis*-decahydro-2-naphthol ($[\alpha]_D^{25} = +32.3^\circ$) from this resolution was calculated to be 80% $[\alpha]_D^{25} = +40.4^\circ$ from the literature [20]. (2*S*,4a*R*,8a*S*)-(−)-*cis*,*cis*-decahydro-2-naphthol was obtained from the basic hydrolysis (0.1 M KOH) of (2*S*)-(−)-*cis*,*cis*-decahydro-2-naphthyl acetate in ethanol in 99% yield. The optical purity of (2*S*,4a*R*,8a*S*)-(−)-*cis*,*cis*-decahydro-2-naphthol ($[\alpha]_D^{25} = -32.7^\circ$) from this resolution was calculated to be 81% ($[\alpha]_D^{25} = -40.4^\circ$ from the literature).

The enantiomeric excess (e.e.) values of (2*R*,4a*S*,8a*R*)-(+)- and (2*S*,4a*R*,8a*S*)-(−)- *cis*,*cis*-decahydro-2-naphthols from the resolutions were calculated to be 78% and 80%, respectively, from the ^{19}F NMR spectra of their Mosher's esters (Figure 3b and Table 1).

In a NMR tube, the condensation reaction of (2*R*,4a*S*,8a*R*)-(+)-*cis*,*cis*- decahydro-2-naphthol (5 mM) with the Mosher's chiral-derivatizing agent (*S*)-(+)-α-methoxy-α-trifluoro-methylphenylacetyl chloride [23] (5 mM) in $CDCl_3$ in the presence of pyridine (5 mM) at 25°C for 24 h. The fluorine chemical shifts at −73.982 and −74.237 ppm with the integration ratio of 89/11 were assigned to be the fluorine atoms of (2*R*,4a*S*,8a*R*)-and (2*S*,4a*R*,8a*S*)- *cis*,*cis*-decahydro-2-naphthyl-(*S*)-α-methoxy-α-trifluoromethyl-phenyl acetates, respectively (Figure 3b) [24,25]. Therefore, the enantiomeric excess of (2*R*,4a*S*,8a*R*)-(+)-*cis*,*cis*-decahydro-2-naphthol from the kinetic resolution by lipase catalysis (Figure 3b) was calculated to be 78% from integration of these two peaks (Table 1).

(2*S*,4a*R*,8a*S*) - (−) - *cis*,*cis* - decahydro - 2 - naphthol (5 mM) was condensed with the Mosher's chiral-derivatizing agent (*S*)-(+)-α-methoxy-α-trifluoro-methylphenylacetyl chloride [23] (5 mM) in $CDCl_3$ in the presence of pyridine (5 mM) at 25°C for 24 h. The fluorine chemical shifts at −74.024 and −74.279 ppm with the integration ratio of 10/90 were assigned to be the fluorine atoms of (2*R*,4a*S*,8a*R*) - and (2*S*,4a*R*,8a*S*) - *cis*,*cis* - decahydro-2-naphthyl - (*S*)-α-methoxy-α-rifluoromethylphenyl acetates, respectively. Therefore, the enantiomeric excess

TABLE 1. Enantiomeric Excess and Optical Purity for the Kinetic Resolution of Enantiomers of *cis*,*cis*-decahydro-2-Naphthanol (Figure 1) by Lipase in Organic Solvent

Compound	*Enantiomeric Excess (%)*[a]	*Optical Purity (%)*[b]
(2*R*,4a*S*,8a*R*)-(+)-*cis*,*cis*-decahydro-2-naphthol	78	80
(2*S*,4a*R*,8a*S*)-(−)-*cis*,*cis*-decahydro-2-naphthol	80	81

[a] Enantiomeric excess (%) was calculated from the ratio of integration of fluorine chemical shifts of their Mosher's ester derivatives of ^{19}F NMR spectra.
[b] Optical purity (%) was calculated as $100 \times [\alpha]_{D\ \text{observed}}^{25} / [\alpha]_{D\ \text{literature}}^{25}$.

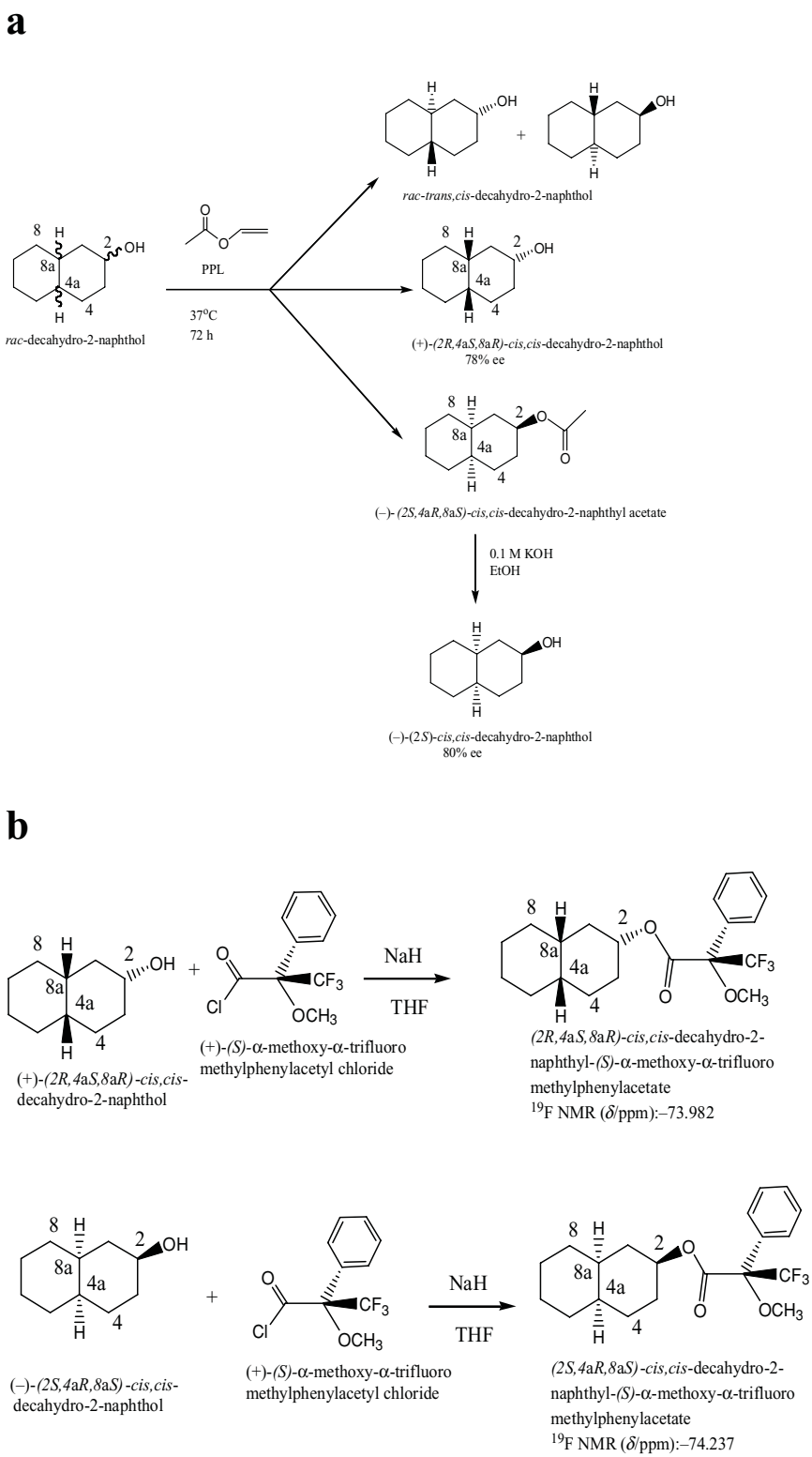

FIGURE 3. (a) Kinetic resolution of (2*S*,4a*R*,8a*S*)-(−)- and (2*R*,4a*S*,8a*R*)-(+)-*cis*,*cis*-decahydro-2-naphthols from lipase-catalyzed acetylation of racemic (±)-*cis*,*cis*-decahydro-2-naphthol with vinyl acetate and (b) determination of enantiomeric excess and absolute configuration of (2*S*,4a*R*,8a*S*)-(−)- and (2*R*,4a*S*,8a*R*)-(+)-*cis*,*cis*-decahydro-2-naphthols by ^{19}NMR spectra of their Mosher's ester derivatives. ^{19}F NMR spectra after the reaction of with S-(+)-α-methoxy-α-trifluoro-methylphenylacetyl chloride in the presence of pyridine in $CDCl_3$. The peaks at −73.982 and −74.237 ppm were assigned to be the fluorine chemical shifts of (2*R*,4a*S*,8a*R*)- and (2*S*,4a*R*,8a*S*)-*cis*,*cis*-(S)-α-methoxy-α-trifluoromethyl-phenylacetates, respectively.

of (2*S*,4a*R*,8a*S*)-(−)-*cis*,*cis*-decahydro-2- naphthol from the kinetic resolution by lipase catalysis was calculated to be 80% from integration of these two peaks (Table 1).

(2R,4aS,8aR)-(+)- or (2S,4aR,8aS)-(−)-, or racemic (±)-cis,cis-decahydro-2-naphthol. ^{1}H NMR ($CDCl_3$) δ0.80–1.80 (m, 16H, 1,3–8,4a,8a-decahydro-2-naphthyl *H*s), 3.07 (m, 1H, decahydro-2-naphthyl-C(2)*H*). ^{13}C NMR ($CDCl_3$) δ 22.5 (*C*-4), 26.2, 26.4 (*C*-6 and *C*-7), 30.6, 30.9 (*C*-5 and *C*-8), 32.0 (*C*-8a), 32.8 (*C*-3), 34.3, 34.7 (*C*-1 and *C*-4a), 74.0 (*C*-2). Mass spectra, exact mass: 154.1354; elemental analysis: calculated for $C_{10}H_{18}O$: C, 77.87; H, 11.76, found C, 77.78; H, 11.93.

(2S,4aR,8aS)-cis,cis-Decahydro-2-naphthylacetate. ^{1}H NMR ($CDCl_3$) δ 0.80–1.80 (m, 16H, 1,3–8,4a,8a-decahydro-2-naphthyl *H*s), 2.00 (s, 3H, acetyl methyl), 3.90 (m, 1H, decahydro-2-naphthyl-C(2)*H*). ^{13}C NMR ($CDCl_3$) δ 17.7 (acetyl methyl), 22.6 (*C*-4), 26.3, 26.4 (*C*-6 and *C*-7), 30.5, 30.8 (*C*-5 and *C*-8), 32.0 (*C*-8a), 32.7 (*C*-3), 34.2, 34.7 (*C*-1 and *C*-4a), 70.1 (*C*-2), 170.9 (acetyl *C*=O). Mass spectra, exact mass: 196.1460; elemental analysis: calculated for $C_{12}H_{20}O_2$: C, 73.43; H, 10.27, found C, 73.31; H, 10.34.

Synthesis of Racemic trans,cis-, (2R,4aS,8aR)-cis,cis-, and (2S,4aR,8aS)-cis,cis-decahydro-2-naphthyl-N-n-butylcarbamates. Racemic *trans*,*cis*-, (2*R*,4a*S*,8a*R*)-*cis*,*cis*-, (2*S*,4a*R*,8a*S*)-*cis*,*cis*-, and racemic *cis*,*cis*-decahydro-2-naphthyl-N-*n*-butylcarbamates (Figure 1) were synthesized from condensation of the corresponding alcohol with *n*-butyl isocyanate in the presence of trethylamine in CH_2Cl_2 for 48 h at 25°C (70–80% yield).

Racemic (±)-trans,cis-decahydro-2-naphthyl-N-n-butylcarbamate. ^{1}H NMR (200 MHz, $CDCl_3$) δ0.92 (*t*, *J* = 7 Hz, 3H, carbamate ω-C*H*$_3$), 1.20–2.00 (m, 20H, carbamate β- and γ-C*H*$_2$ and decahydro-2-naphthyl *H*s), 3.17 (dt, *J* = 6 and 7 Hz, 2H, carbamate α-C*H*$_2$), 3.88 (m, 1H, decahydro-2-naphthyl C(2)-*H*), 4.53 (br. s, 1H, carbamate NH).

^{13}C NMR (50.3 MHz, $CDCl_3$) δ 13.7 (carbamate ω-CH_3), 19.9 (carbamate β-CH_2), 26.5, 22.6, 28.2, 30.3, 32.1, 33.7 (decahydro-2-naphthyl *C*-3 to *C*-8), 33.7 (carbamate γ-CH_2), 37.2 (decahydro-2-naphthyl *C*-9), 37.6 (decahydro-2-naphthyl *C*-1), 40.6 (decahydro-2-naphthyl *C*-10), 42.7 (carbamate α-CH_2), 70.4 (decahydro-2-naphthyl *C*-2), 156.4 (carbamate *C*=O).

(2R,4aS,8aR)-, (2S,4aR,8aS)-, or Racemic cis,cis-decahydro-2-naphthyl- N-n-butylcarbamate. ^{1}H NMR (200 MHz, $CDCl_3$) δ 0.92 (*t*, *J* = 7 Hz, 3H, carbamate ω-C*H*$_3$), 1.20–2.00 (m, 20H, carbamate β- and γ-C*H*$_2$ and decahydro-2-naphthyl *H*s), 3.15 (dt, *J* = 6 and 7 Hz, 2H, carbamate α-C*H*$_2$), 4.56 (m, 1H, decahydro-2-naphthyl C(2)-*H*), 4.84 (br. s, 1H, carbamate NH).

^{13}C NMR (50.3 MHz, $CDCl_3$) δ 13.6 (carbamate ω-CH_3), 19.7 (carbamate β-CH_2), 26.4, 31.3, 33.0, 33.6, 34.4, 35.2 (decahydro-2-naphthyl *C*-3 to *C*-8), 32.0 (carbamate γ-CH_2), 38.5 (decahydro-2-naphthyl *C*-1), 40.6 (decahydro-2-naphthyl *C*-9), 40.9 (carbamate α-CH_2), 42.2 (decahydro-2-naphthyl *C*-10), 73.2 (decahydro-2-naphthyl *C*-2), 156.3 (carbamate *C*=O).

Instrumental Methods

All steady-state kinetic data were obtained from a UV–visible spectrometer (Agilent 8453) with a cell holder circulated with a water bath.

Data Reduction and Molecular Modeling

Origin (version 6.0) was used for the linear and nonlinear least-squares curve fittings. Molecular structures shown in figures were depicted from the molecular structures after MM-2 energy minimization (minimum root mean square gradient was set to be 0.01) by CS Chem 3D (version 6.0).

AChE and BChE Inhibitions

The inhibition reactions of AChE and BChE were determined by the Ellman assay [26]. The AChE-catalyzed hydrolysis of acetylthiocholine (0.1 mM) or BChE-catalyzed hydrolysis of butyrylthiocholine (0.1 mM) in the presence of 5,5′-dithio-bis(2-nitrobenzoic acid) (0.1 mM) and inhibitors were followed continuously at 410 nm on a UV–visible spectrometer at 25°C, pH 7.1. The K_i and k_2 values were parameters obtained from the nonlinear least squares of curve fittings of the k_{app} values vs. inhibition concentration ([I]) plot following Eq. (2) (Figure 4 and Tables 2 and 3).

Statistics

Errors of K_i and k_2 values (Tables 2 and 3) were depicted as the errors of parameters from the nonlinear least squares of curve fittings of the k_{app} values vs. inhibition concentration ([I]) plot following Eq. (1) by Origin (version 6.0). Errors of k_i values were depicted as the followings:

$$\text{Error of } k_i = (\text{Error of } K_i)^2 + (\text{Error of } k_2)^2)^{1/2}$$

RESULTS AND DISCUSSION

(2*S*,4a*R*,8a*S*)-*cis*,*cis*-, (2*R*,4a*S*,8a*R*)-*cis*,*cis*-, racemic *cis*,*cis*-, and racemic *trans*,*cis*-decahydro-2-naphthyl-N-*n*-butylcarbamates (Figure 1) were synthesized from

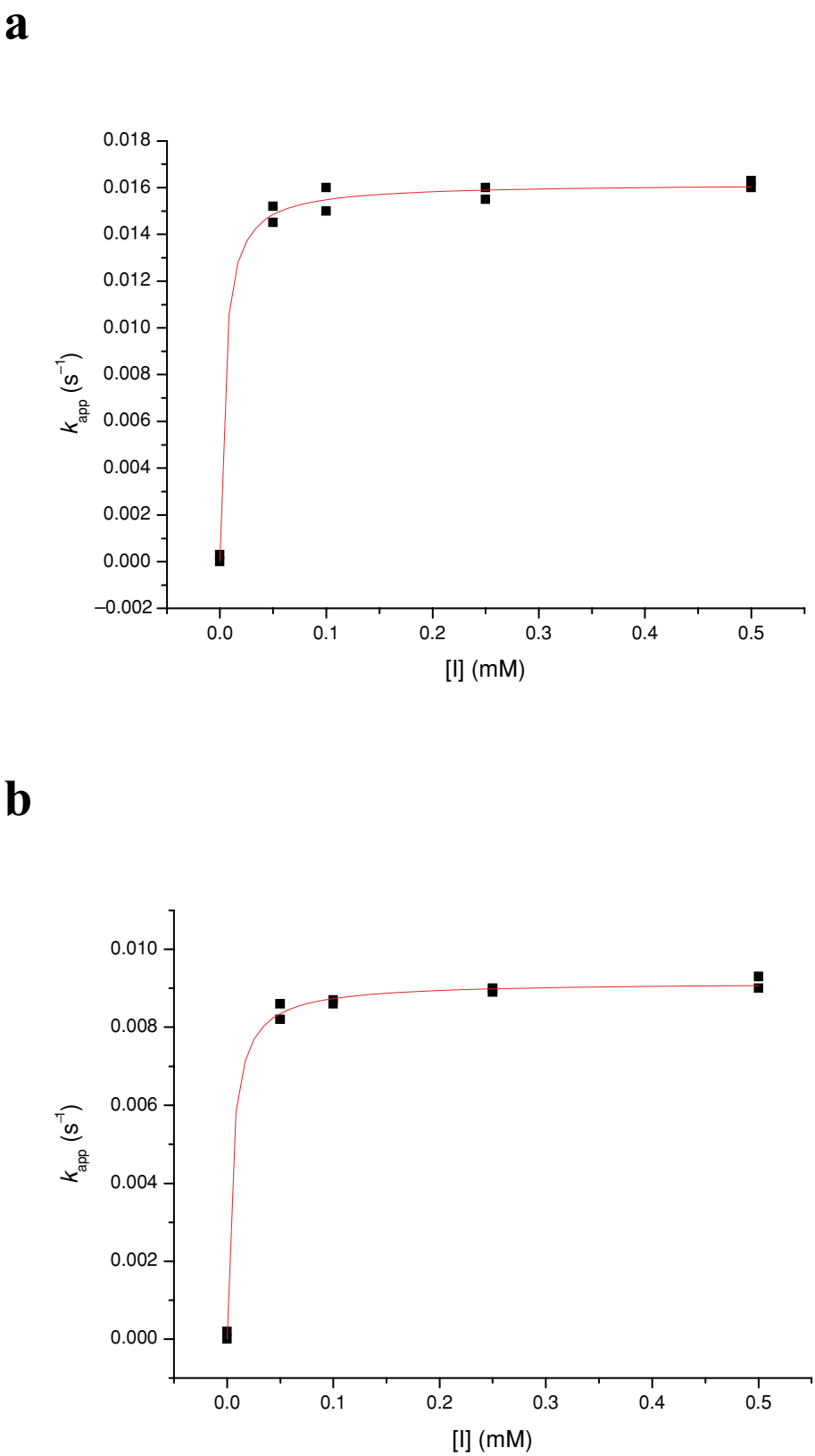

FIGURE 4. Nonlinear least-squares curve fittings of k_{app} vs. inhibitor concentration ([I]) plots against Eq. (1) for the pseudosubstrate inhibitions [8] of (a) AChE and (b) BChE by (2*R*,4a*S*,8a*R*)-*cis*,*cis*-decahydro-2-naphthyl- N-*n*-butylcarbamate. The parameters of the fit were (a) $k_2 = 0.0167 \pm 0.00001$ s^{-1}, $K_i = 2.2 \pm 0.6$ μM, and $R = 0.9972$ and (b) $k_2 = 0.0091 \pm 0.0001$ s^{-1}, $K_i = 2.4 \pm 0.5$ μM, and $R = 0.99828$.

TABLE 2. k_2, K_i, and k_i Values[a] of the AChE Inhibitions by Stereoisomers of Decahydro-2-naphthyl N-*n*-butylcarbamates

Inhibitors[b]	$K_i(\mu M)$	$k_2(10^{-2}s^{-1})$	$k_i(10^3\ M^{-1}s^{-1})$	*Enantioselectivity*
rac-(±)-*trans,cis*	3.5 ± 0.3	0.40 ± 0.04	1.1 ± 0.1	–
(2*R*,4a*S*,8a*R*)-*cis,cis*-	2.2 ± 0.6	1.67 ± 0.02	8 ± 2	2.4
(2*S*,4a*R*,8a*S*)-*cis,cis*-	6.0 ± 0.6	2.0 ± 0.2	3.3 ± 0.5	1.0
rac-(±)-*cis,cis*-	4 ± 1	2.0 ± 0.1	5 ± 1	1.5

[a] Obtained from the nonlinear least-squares curve fittings of k_{app} vs. [I] plot against Eq. (1) (Figure 4a).

[b] (2*R*,4a*S*,8a*R*)-*cis,cis*-, (2*S*,4a*R*,8a*S*)-*cis,cis*-, and *rac*-(±)-*cis,cis*- stand for (2*R*,4a*S*,8a*R*)-, (2*S*,4a*R*,8a*S*)-, and racemic *cis,cis*-decahydro-2-naphthyl-N-*n*-butylcarbamates. *rac*-(±)-*trans,cis* stand for (2*R*,4a*S*,8a*S*)- and (2*S*,4a*R*,8a*R*)-*trans,cis*-decahydro-2-naphthyl-N-*n*-butylcarbamates.

the corresponding alcohols to study the stereospecificity of AChE and BChE inhibitions.

Superimposition of (2*S*,4a*R*,8a*S*)-(−)- and (2*R*,4a*S*,8a*R*)-(+)-*cis,cis*-decahydro -2-naphthols into the active site of acetyl enzyme suggests that the decahydro-2-naphthyl ring of (2*S*,4a*R*,8a*S*)-(−)- *cis,cis*-decahydro-2-naphthol fits well into the leaving group binding site of the enzyme and the hydroxyl group of (2*S*,4a*R*,8a*S*)-(−)- *cis,cis*-decahydro-2-naphthol is at the right position to attack the carbonyl carbon of acetyl enzyme (Figure 5a). On the other hand, the decahydro-2-naphthyl ring of (2*R*,4a*S*,8a*R*)-(+)-*cis,cis*-decahydro-2-naphthol does not fit well into the leaving group binding site of the enzyme, extending to the entrance (mouth) of the active site. Thus, the hydroxyl group of (2*R*,4a*S*,8a*R*)-(+)-*cis,cis*-decahydro-2-naphthol is away from the right position to attack the acetyl enzyme.

(2*S*,4a*R*,8a*S*)-*cis,cis*-, (2*R*,4a*S*,8a*R*)-*cis,cis*-, racemic *cis,cis*-, and racemic *trans,cis*-decahydro-2-naphthyl-N-*n*-butylcarbamates (Figure 1) are all characterized as pseudosubstrate inhibitors of AChE and BChE (Eq. (1), Figure 2, Tables 2 and 3) [8–15,17,19,27–30].

For stereospecificity of the AChE inhibition by enantiomers of *cis,cis*-decahydro-2- naphthyl-N-*n*-butylcarbamates, (2*R*,4a*S*,8a*R*)-*cis,cis*-isomer is 2.4 times more potent than (2*S*,4a*R*,8a*S*)-*cis,cis*-isomer (Table 2). This stereopreference ($R > S$) is the same with that for the inhibition by enantiomers of *exo*-2-norbornyl-N-*n*-butylcarbamate but is opposite to that for the inhibition by enantiomers of *endo*-2-norbornyl-N-*n*-butylcarbamate [17].

Superimposition of both enantiomers of *cis,cis*-decahydro-2-naphthyl-N-*n*- butylcarbamate into the active site of AChE indicates that the decahydro-2-naphthyl rings of (2*S*,4a*R*,8a*S*)-*cis,cis*-isomer is strongly repulsive with the anionic substrate binding site of AChE [1–3], suggesting that this unfavorable interaction makes (2*S*,4a*R*,8a*S*)-*cis,cis*-inhibitor less impotent (Figure 5b). On the other hand, the decahydro-2-naphthyl rings of (2*R*,4a*S*,8a*R*)-*cis,cis*-inhibitor does not have such unfavorable repulsions.

Comparison between racemic *cis,cis*- and racemic *trans,cis*-decahydro-2-naphthyl-N-*n*- butylcarbamates for AChE inhibition reveals that the former is more potent than the latter (Table 2) probably due to the fact that the decahydro-2-naphthyl ring of *trans,cis*-inhibitor is repulsive to the anionic substrate binding site of the enzyme and that this repulsion weakens the binding between *trans,cis*-inhibitor and the enzyme (Figure 5b).

For stereospecificity of the BChE inhibition by *cis,cis*-decahydro-2- naphthyl-N-*n*-butylcarbamates, (2*R*,4a*S*,8a*R*)-*cis,cis*-inhibitor is 2.7 times more potent than (2*S*,4a*R*,8a*S*)-*cis,cis*-inhibitor (Table 3).

Superimposition of both the enantiomers of *cis,cis*-decahydro-2-naphthyl-N-*n*- butylcarbamate into the active site of BChE indicates that the decahydro-2-naphthyl rings of (2*S*,4a*R*,8a*S*)-*cis,cis*-isomer is strongly repulsive with the anionic substrate-binding site of BChE [4–7], suggesting that this unfavorable interaction makes (2*S*,4a*R*,8a*S*)-*cis,cis*-inhibitor less impotent (Figure 5c). On the other hand, the decahydro-2-naphthyl rings of (2*R*,4a*S*,8a*R*)-*cis,cis*-inhibitor does not have such unfavorable repulsions.

Comparison between racemic *cis,cis*- and racemic *trans,cis*-decahydro-2-naphthyl-N-*n*- butylcarbamates for BChE inhibition reveals that the former is less potent

TABLE 3. k_2, K_i, and k_i Values[a] of the BChE Inhibitions by Decahydro-2-naphthyl N-*n*-butylcarbamates

Inhibitors[b]	$K_i(\mu M)$	$k_2(10^{-3}s^{-1})$	$k_i(10^3\ M^{-1}s^{-1})$	*Enantioselectivity*
rac-(±)-*trans,cis*	3.0 ± 0.2	10.0 ± 0.5	3.3 ± 0.3	–
(2*R*,4a*S*,8a*R*)-*cis,cis*-	2.4 ± 0.5	9.1 ± 0.1	3.8 ± 0.8	2.7
(2*S*,4a*R*,8a*S*)-*cis,cis*-	5.0 ± 0.8	7.0 ± 0.3	1.4 ± 0.2	1.0
rac-(±)-*cis,cis*-	4.0 ± 0.5	9.0 ± 0.4	2.0 ± 0.3	1.4

[a] Obtained from the nonlinear least-squares curve fittings of k_{app} vs. [I] plot against Eq. (1) (Figure 4b).

[b] (2*R*,4a*S*, 8a*R*)- *cis,cis*-, (2*S*,4a*R*,8a*S*)-*cis,cis*-, and *rac*-(±)-*cis,cis*- stand for (2*R*,4a*S*,8a*R*)-, (2*S*,4a*R*,8a*S*)-, and racemic *cis,cis*-decahydro-2-naphthyl-N-*n*-butylcarbamates. *rac*-(±)-*trans,cis* stand for (2*R*,4a*S*,8a*S*)- and (2*S*,4a*R*,8a*R*)-*trans,cis*-decahydro-2-naphthyl-N-*n*-butylcarbamates.

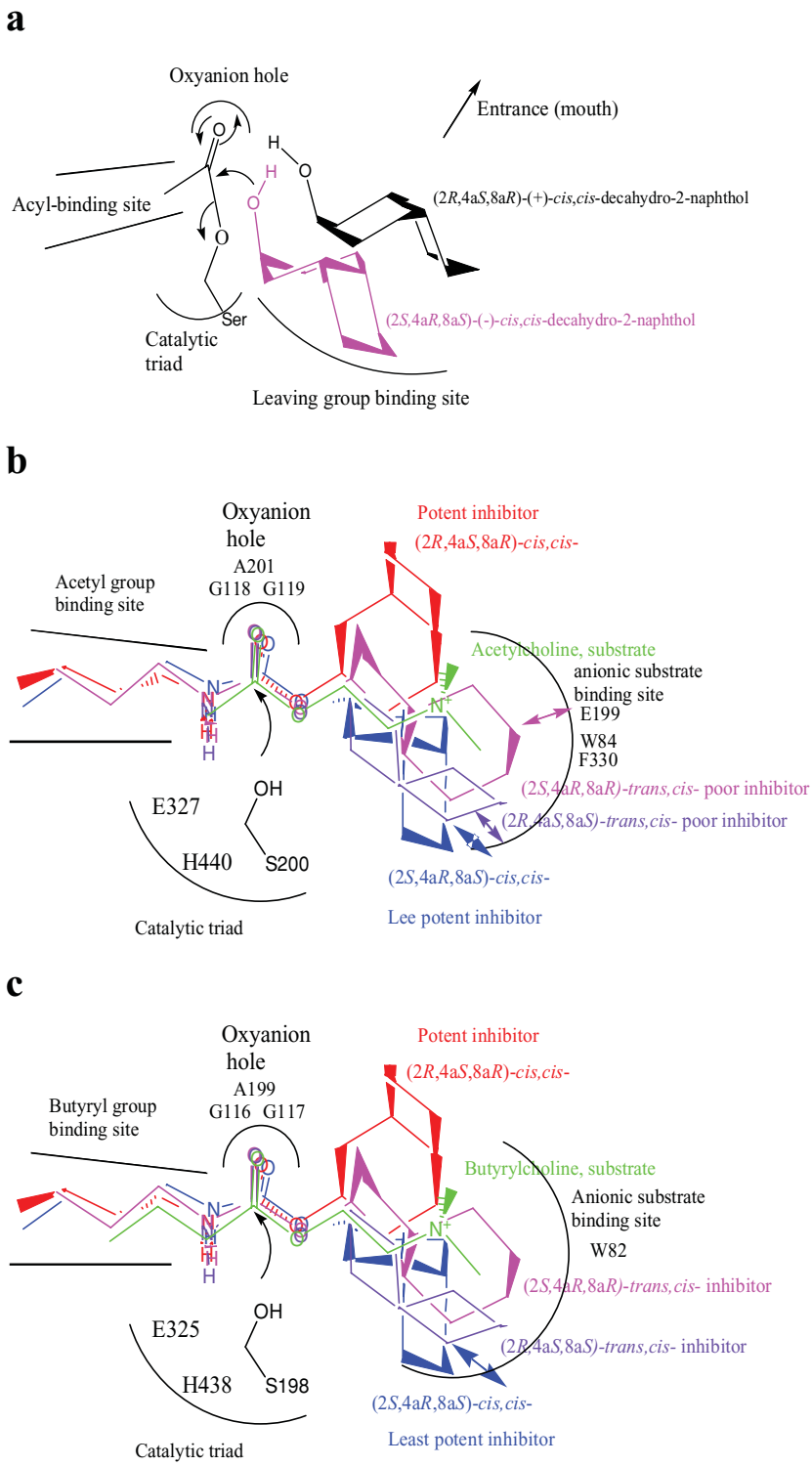

FIGURE 5. (a) Superimposition of (2*S*,4a*R*,8a*S*)-(−)- and (2*R*,4a*S*,8a*R*)-(+)- *cis*,*cis*-decahydro-2-naphthols into the active site of acetyl lipase; (b) superimposition of (2*S*,4a*R*,8a*S*)-*cis*,*cis*-, (2*R*,4a*S*,8a*R*)-*cis*,*cis*-, (2*S*,4a*R*,8a*R*)-*trans*,*cis*-, (2*R*,4a*S*,8a*S*)-*trans*,*cis*-decahydro-2-naphthyl- N-*n*-butylcarbamates into the active site of AChE [1–3]. The decahydro-2-naphthyl ring of (2*S*,4a*R*,8a*S*)-*cis*,*cis*- and racemic-trans,cis-inhibitors strongly repulse the anionic substrate binding site of the enzyme, but that of (2*R*,4a*S*,8a*R*)-inhibitor does not have such repulsion and fits well into the anionic substrate binding site; (c) superimposition of (2*S*,4a*R*,8a*S*)-*cis*,*cis*-, (2*R*,4a*S*,8a*R*)-*cis*,*cis*-, (2*S*,4a*R*,8a*R*)-*trans*,*cis*-, (2*R*,4a*S*,8a*S*)-*trans*,*cis*-decahydro-2-naphthyl-N-*n*-butylcarbamates into the active site of BChE [4–7]. The decahydro-2-naphthyl ring of (2*S*,4a*R*,8a*S*)-*cis*,*cis*-inhibitor strongly repulses the anionic substrate binding site of the enzyme, but those of (2*R*,4a*S*,8a*R*)- and racemic-trans,cis-inhibitors do not have such repulsion and fit well into the anionic substrate binding site.

than the latter (Table 3). This stereopreference (trans,cis > cis,cis) is opposite to that for AChE inhibition. This result indicates that the anionic substrate-binding site of BChE is relatively larger than that of AChE (Figure 5c). Therefore, the anionic substrate-binding site of BChE is large enough to bind to the decahydro-2-naphthyl ring of trans,cis-inhibitor. Thus, the unfavorable repulsion between the anionic substrate-binding site of AChE and the decahydro-2-naphthyl ring of trans,cis-inhibitor (Figure 5b) does not happen in the BChE inhibition (Figure 5c).

In summary, optically pure (2*S*,4a*R*,8a*S*)-(−)- and (2*R*,4a*S*,8a*R*)-(+)-*cis*,*cis*- decahydro-2-naphthols are resolved from the lipase-catalyzed acetylation reaction. For both AChE and BChE inhibitions, (2*S*,4a*R*,8a*S*)-*cis*,*cis*-decahydro-2-naphthyl-N-*n*-butylcarbamate is a more potent inhibitor than (2*R*,4a*S*,8a*R*)-*cis*,*cis*-decahydro- 2-naphthyl-N-*n*-butylcarbamate.

REFERENCES

1. Quinn DM. Acetylcholinesterase: enzyme structure, reaction dynamics, and virtual transition states. Chem Rev 1987;87:955–979.
2. Sussman JL, Harel M, Frolow F, Oefner C, Goldman A, Toker L, Silman I. Atomic structure of acetylcholinesterase from *Torpedo californica*: a prototypic acetylcholine-binding protein. Science 1991;253:872–879.
3. Bar-On P, Millard CB, Harel M, Dvir H, Enz A, Sussman JL, Silman I. Kinetic and structural studies on the interaction of cholinesterase with anti-Alzheimer drug Rivastigmine. Biochemistry 2002;41:3555–3564.
4. Masson P, Froment M-T, Fort S, Ribes F, Bec N, Balny C, Schopfer LM. Butyrylcholinesterase-catalyzed hydrolysis of *N*-methylindoxyl acetate: analysis of volume changes upon reaction and hysteretic behavior. Biochim Biophys Acta 2002;1597:229–243.
5. Loudwig S, Nicolet Y, Masson P, Fontecilla-Camps JC, Bon S, Nachon F, Goeldner M. Photoreversible inhibition of cholinesterase: catalytic serine-labeled caged butyrylcholinesterase. ChemBioChem 2003;4:762–767.
6. Savini L, Gaeta A, Fattorusso C, Catalanotti B, Campiani G, Chiasserini L, Pellerano C, Novellino E, McKissic D, Saxena A. Specific targeting of acetylcholinesterase and butyrylcholinesterase recognition sites. Rational design of novel, selective, and highly potent cholinesterase inhibitors. J Med Chem 2003;46:1–4.
7. Nicolet Y, Lockridge O, Masson P, Fontecilla-Camps JC, Nachon F. Crystal structure of human butyrylcholinesterase and of its complexes with substrate and products. J Biol Chem 2003;278:41141–41147.
8. Hosie L, Sutton LD, Quinn DM. *p*-Nitrophenyl and cholesteryl-*N*-alkyl carbamates as inhibitors of cholesterol esterase. J Biol Chem 1987;262:260–264.
9. Lin G, Lai C-Y. Hammett analysis of the inhibition of pancreatic cholesterol esterase by substituted phenyl-*N*-butylcarbamate. Tetrahedron Lett 1995;36:6117–6120.
10. Lin G, Lai C-Y. Linear free energy relationships of the inhibition of pancreatic cholesterol esterase by 4-nitrophenyl-*N*-alkylcarbamate. Tetrahedron Lett 1996;37:193–196.
11. Lin G, Chen G-H, Ho H-C. Conformationally restricted carbamate inhibitors of horse serum butyrylcholinesterase. Bioorg Med Chem Lett 1998;8:2747–2750.
12. Lin G, Lai C-Y, Liao W-C. Molecular recognition by acetylcholinesterase at the peripheral anionic site: structure-activity relationships for inhibitions by aryl carbamates. Bioorg Med Chem 1999;7:2683–2689.
13. Lin G, Shieh C-T, Ho H-C, Chouhwang J-Y, Lin W-Y, Lu C-P. Structure-reactivity relationships for the inhibition mechanism at the second alkyl-chain-binding site of cholesterol esterase and lipase. Biochemistry 1999;38:9971–9981.
14. Lin G, Lai C-Y, Liao W-C, Kuo B-H, Lu C-P. Structure–reactivity relationships as probes for the inhibition mechanism of cholesterol esterase by aryl carbamates. I. Steady-state kinetics. J Chin Chem Soc 2000;47:489–500.
15. Lin G, Chouhwang J-Y. Quantitative structure–activity relationships for the inhibition of *Pseudomonas* species lipase by 4-nitrophenyl-*N*-substituted carbamates. J Biochem Mol Biol Biophys 2001;5:301–308.
16. Lin G, Tsai Y-C, Liu H-C, Liao W-C, Chang C-H. Enantiomeric inhibitions of cholesterol esterase and acetylcholinesterase. Biochim Biophys Acta 1998;1388:161–174.
17. Chiou S-Y, Huang C-F, Yeh S-J, Chen I-R, Lin G. Synthesis of enantiomers of *exo*-2-norbornyl-N-*n*-butylcarbamate and *endo*-2-norbornyl-N-*n*-butylcarbamate for stereoselective inhibition of acetylcholinesterase. Chirality 2010;22:267–274.
18. Doorn JA, Talley TT, Thompson CM, Richardson RJ. Probing the active sites of butyrylcholinesterase and cholesterol esterase with isomalathion: conserved stereoselective inactivation of serine hydrolases structurally related to acetylcholinesterase. Chem Res Toxicol 2001;14:807–813.
19. Chiou S-Y, Huang C-F, Yeh S-J, Chen I-R, Lin G. Stereoselective inhibition of butyrylcholinesterase by enantiomers of *exo*- and *endo*-norbornyl-N-*n*-butylcarbamates. J Enzym Inhib Med Chem 2010;25:13–20.
20. Oritani T, Yamashita K, Kabuto C. Enantioselectivity of microbial hydrolysis of (±)-decahydro-2-naphthyl acetates. Preparations and absolute configurations of chiral decahydro-2-naphthols. J Org Chem 1984;49:3689–3694.
21. Boland W.; Frößl C, Lorenz N. Esterolytic and lipolytic enzymes in organic synthesis. Synthesis 1991;12:1049–1072.
22. Theil F. Lipase-supported synthesis of biologically active compounds. Chem Rev 1995;95:2203–2227.
23. Dale JA, Mosher HS. Nuclear magnetic resonance enantiomer reagents. Configurational correlations via nuclear magnetic resonance chemical shifts of diastereomeric mandelate, *o*-methylmandelate, and α-methoxy-α-trifluoromethylphenylacetate (MTPA) esters. J Am Chem Soc 1973;95:512–519.
24. Takahashi T, Fukuishima A, Tanaka Y, Takeuchi Y, Kabuto K, Kabuto C. CFTA, a new efficient agent for determination of absolute configurations of chiral secondary alcohols. Chem Commun 2000:788–789.
25. Takahashi T, Kameda H, Kamei T, Ishizaki M. Synthesis of 1-fluoroindan-1-carboxylic acid (FICA) and its properties as a chiral derivatizing agent. J Fluorine Chem 2006;127:760–768.

26. Ellman CL, Courtney KD, Andres VJ, Featherstone RM. A new rapid colorimetric determination of acetylcholinesterase activity. Biochem Pharm 1961;7:88–95.
27. Feaster SR, Lee K, Baker N, Hui DY, Quinn DM. Molecular recognition by cholesterol esterase of active site ligands: structure-reactivity effects for inhibition by aryl carbamates and subsequent carbamylenzyme turnover. Biochemistry 1996;35:16723–16734.
28. Feaster SR, Quinn DM. Mechanism-based inhibitors of mammalian cholesterol esterase. Methods Enzymol 1997;286:231–252.
29. Pietsch M, Gütschow M. Alternate substrate inhibition of cholesterol esterase by thieno[2,3-*d*][1,3]oxazin-4-ones. J Biol Chem 2002;277:24006–24013.
30. Pietsch M, Gütschow M. Syntehsis of tricyclic 1,3-oxazin-4-ones and kinetic analysis of cholesterol esterase and acetylcholinesterase inhibition. J Med Chem 2005;48:8270–8288.